J. Am. Soc. Mass Spectrom. (2019) 30:2007–2013
DOI: 10.1007/s13361-019-02218-2

FOCUS: HONORING HELMUT SCHWARZ'S ELECTION TO THE NATIONAL ACADEMY OF SCIENCES: RESEARCH ARTICLE

[2.2]Paracyclophane bis(pyridine)-based metallosupramolecular rhombs in the gas phase: Competitive cleavage of non-covalent and weak covalent bonds

Yvonne Lorenz, Jana Anhäuser, Arne Lützen, Marianne Engeser

Kekulé-Institute of Organic Chemistry and Biochemistry, University of Bonn, Gerhard-Domagk-Str. 1, 53121, Bonn, Germany

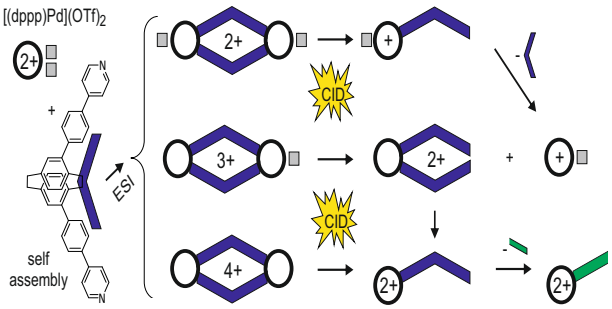

Abstract. The gas-phase fragmentation behavior of self-assembled metallo-supramolecular rhombs based on an unusual chiral [2.2]paracyclophane bis(pyridine) ligand is studied by collision-induced dissociation mass spectrometry. The fragmentation patterns strongly depend on the charge state of the respective mass-selected aggregate. For the doubly charged ions, simple symmetric fragmentation is observed in full accordance with previous results reported for related metallo-supramolecular species. The triply charged species cleaves unsymmetrically which can be rationalized by a preferred formation of ions with low charge density. CID of the quadruply charged rhomb reveals a complex fragmentation. Besides ligand oxidation to the radical cation, facile cleavage of the central covalently bound part of the [2.2]paracyclophane ligand takes place which is even preferred over rupture of the weak dative pyridine-Pd bond.

Keywords: Metallo-supramolecular chemistry, Weak covalent bonds, Chiral, Collision-induced dissociation, Self-assembly, Rhombs

Received: 28 February 2019/Revised: 3 April 2019/Accepted: 7 April 2019/Published Online: 16 May 2019

Introduction

Self-assembly has lead to numerous fascinating supramolecular structures and functional architectures based on an impressive variety of subcomponents. One way to design self-assembly processes uses the metallo-supramolecular approach based on well-chosen organic ligands interconnecting two or more metal centers [1–6]. Aggregate formation is thus based on weak reversible dative bonds long established in coordination chemistry. There are impressive examples in literature of highly selective self-assembly processes of multicomponent mixtures [1–6] even leading to complex heterometallic assemblies [7–10]. However, predicting the outcome of self-assembly in such systems is still a challenge [11–14]. To obtain a single species instead of a statistical mixture, the electronic and steric demands of all building blocks need to be adjusted very carefully to avoid unwanted interferences [15–17]. A successful design thus needs a solid knowledge of the size, shape, flexibility, and of the dynamic behavior and interactions of the subcomponents chosen to build the aggregate.

Mass spectrometry has become an indispensable tool to determine the stoichiometry of self-assembled aggregates [18–35]. This task however is often very challenging as very soft ionization conditions are needed to avoid in-source fragmentation [18–22], although analysis of the detected fragments can also confirm the structure of the aggregate in fortunate cases [26, 36–40]. Hence, it is tempting to use induced fragmentation [41, 42] in the gas phase to deduce the structure of metallo-supramolecular aggregates in analogy to the well-established

Dedicated to Professor Helmut Schwarz.

Correspondence to: Marianne Engeser; *e-mail:* Marianne.Engeser@uni-bonn.de

routes of structure elucidation of covalent compounds by mass spectrometry [41–43]. However, the combination of rather weak non-covalent bonds that form the aggregate and strong Coulomb interactions between the charged metal centers and between metals and counter anions (which are not shielded in the gas phase in contrast to solution) can result in unforeseen fragmentation pathways and rearrangements that easily can be misleading in structure determination [44]. In our eyes, a much broader experimental basis is currently needed to better understand the gas-phase fragmentation patterns of metallo-supramolecular aggregates and establish fragmentation rules that are useful for structure elucidation of metallo-supramolecular aggregates by mass spectrometric means. In addition, induced fragmentations can also yield information on the relative stability of non-covalent bonds [18–22, 45–50]. Such information is highly valuable as it forms the basis for a rational design of complex functional supramolecular aggregates.

Our gas-phase fragmentation studies of metallo-supramolecular aggregates started with "squares" of the classic Stang-type [51] built out of four identical (elongated) 4,4′-bipyridine ligands and *cis*-protected Pd and Pt complexes with diphenylphosphinopropane (dppp) ligands [52, 53]. Heterobimetallic squares incorporating two different types of metal complexes expectedly exhibit much more complex fragmentation patterns which strongly depend on the ligand length and thus aggregate size [50], whereas metallo-supramolecular rhombs formed out of six metal centers (2× Pt/Pd, 4× Au) showed a very general and simple fragmentation scheme [44]. Due to the pronounced difference in metal-ligand binding energies, the gold complexes did not take part in the fragmentation at all.

We reported on the synthesis of rather rigid racemic and enantiomerically pure planar chiral ligands based on a *pseudo-meta*-difunctionalized [2.2]paracyclophane skeleton and on their self-assembly behavior with a special focus on self-sorting vs. self-discrimination very recently [54]. The combination of the abovementioned (dppp)Pd building block with the chiral enantiomerically pure ligand $L = (R_p)$-4,15-bis(4-(pyridin-4-yl)phenyl)[2.2]paracyclophane yields rhomb-like aggregates (Scheme 1) which could be thoroughly characterized by NMR, X-ray diffraction analysis, and electrospray (ESI) mass spectrometry including accurate mass determination [54]. In the course of this project, we also performed collision-induced dissociation (CID) experiments and noted a peculiar fragmentation behavior which we report herein.

Experimental Section

ESI mass spectra in positive mode were recorded on a commercial micrOTOF-Q quadrupole/time-of-flight mass spectrometer from Bruker Daltonik equipped with its standard ESI source and a Thermo Fisher Scientific LTQ Orbitrap XL™ hybrid mass spectrometer equipped with an IonMax source with a heated electrospray ionization (HESI-II) probe. Acetonitrile solutions in concentrations of approximately 100 µM were used and transferred into the ion source using a syringe pump at flow rates of 5–10 µL/min. Source parameters are individually tuned for best abundances and low amounts of in-source fragmentation for every sample. Typical Q/TOF parameters are as follows: end plate offset, − 500 V; capillary, 4 kV; nebulizer gas (N_2), 5 bar; dry gas (N_2), 1 L/min; dry gas temperature, 20 °C; funnel 1 RF, 280 Vpp; funnel 2, 290 Vpp; ISCID energy, 0 eV; quadrupole ion energy, 1 eV; hexapole RF, 290 Vpp; collision cell energy, 1 eV; and coll. RF, 500 Vpp. In CID experiments at the Q/TOF instrument, the

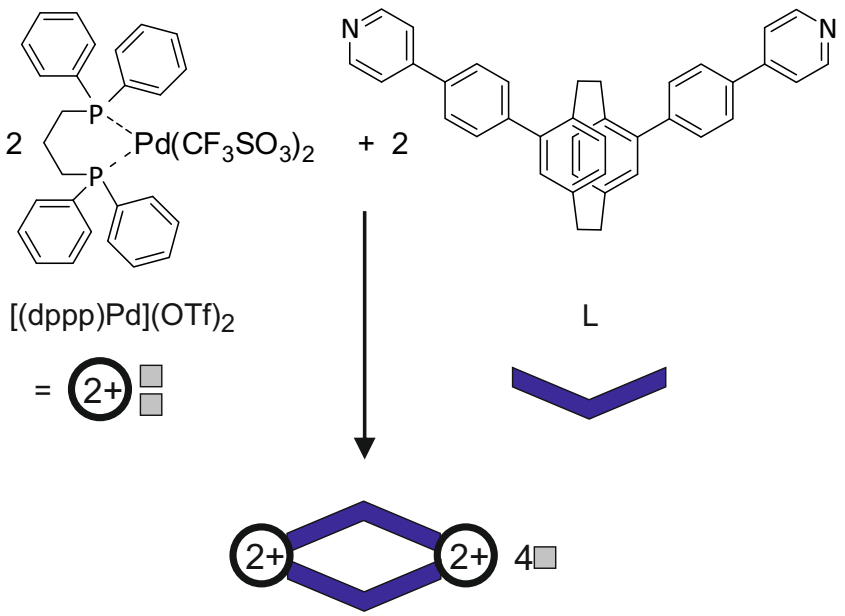

Scheme 1. Formation of $[Pd_2(dppp)_2L_2](OTf)_4$ by self-assembly of $[(dppp)Pd](OTf)_2$ and the [2.2]paracyclophane bis(pyridine)-based ligand L. Here and in the next figures, a gray square indicates a triflate anion, the circled 2+ indicates the $(dppp)Pd^{2+}$ complex fragment and the blue buckled line the ligand L

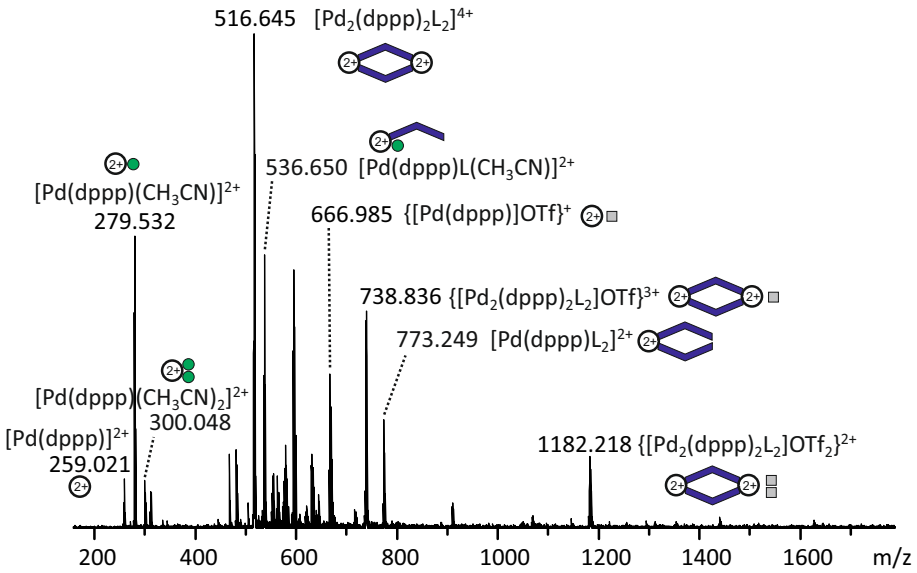

Figure 1. ESI positive mass spectrum of 1:1 mixture of L and $[Pd(dppp)](OTf)_2$ in CD_3CN measured on a Q/TOF mass spectrometer. Green circles symbolize acetonitrile adducts

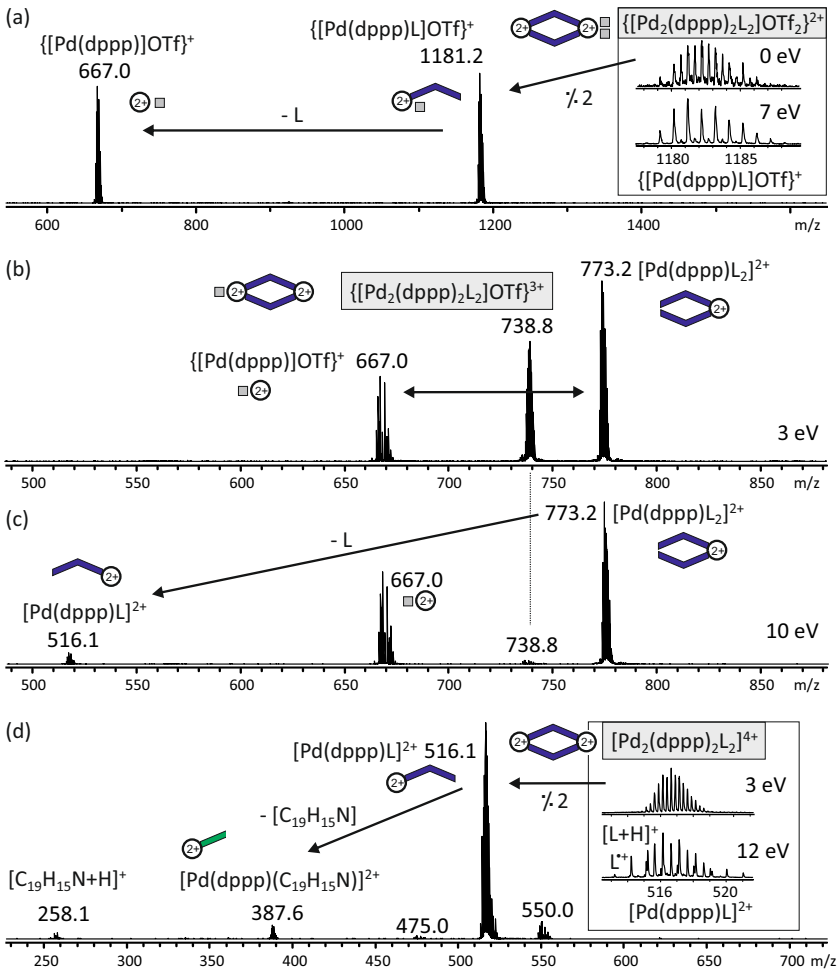

Figure 2. CID-mass spectra for mass-selected ions $[Pd_2(dppp)_2L_2](OTf)_{4-n}]^{n+}$ (highlighted in gray boxes) measured with the Q/TOF mass spectrometer at the indicated collision energy voltages: (**a**) $n = 2$; (**b**) and (**c**) $n = 3$; and (**d**) $n = 4$. The insets show the isotope pattern in the mass-selected region at low collision energy voltage (top) and at the higher value chosen for the shown spectra (bottom). The green line represents a coordinated ligand fragment $C_{19}H_{15}N$ for which a putative structure is given in Figure 4

full isotope pattern was mass-selected and argon was used as collision gas. At the Orbitrap instrument, CID experiments were performed in the He-filled ion trap while ion detection was achieved in the orbitrap analyzer with the resolution set to $R = 30{,}000$.

Results and Discussion

The ESI mass spectra of $[Pd_2(dppp)_2L_2](OTf)_4$ showed the typical signals expected for metallo-supramolecular species: The intact rhombs were detected with correct accurate masses and isotope patterns in a series of different charge states obtained by stripping off two, three, or all four triflate counter ions [54]. Unfortunately, significant amounts of in-source fragmentation occurred additionally under routine ESI conditions at the Orbitrap instrument which we did not achieve to suppress even by tuning the source parameters manually. Fragmentation into smaller ions was much less pronounced at the Q/TOF instrument after careful tuning of the ESI parameters to very soft ionization conditions (Figure 1). Superpositions of the signals for the intact rhombs with signals of fragments could thus be avoided almost completely. This comes however at the cost of significant loss of signal intensity and the appearance of acetonitrile adducts [55].

The detection of non-superimposed signals for intact rhombs made it possible to perform collision-induced dissociation (CID) experiments in a controlled manner after mass-selection of the respective ions of interest. Similar to our previous findings for metallo-supramolecular squares [52, 53], the CID mass spectra of the rhombs differ significantly depending on the charge of the gas-phase aggregate (Figure 2).

The fragmentation behavior observed upon CID of the doubly charged rhombs follows a very simple pattern (Figure 2a): The aggregate splits symmetrically in halves, leading to ions of the same m/z ratio, but with an isotope pattern with full mass spacing indicating a singly charged ion. The resulting mononuclear monoligated complex $\{[Pd(dppp)L](OTf)\}^+$ subsequently loses the neutral ligand L to form the "unligated" metal complex $\{[Pd(dppp)]OTf\}^+$ at m/z 667 followed by expulsion of triflic acid HOTf (see below). This pattern fully matches the behavior of the much larger doubly charged rhombs described previously [44].

The triply charged rhomb behaves differently (Figure 2b). Its fragmentation also separates the charges on two ions, but unsymmetrically: the two ligands L remain bound to the same metal core. Thus, this fragmentation leads to a larger dication at m/z 773 binding both monodentate ligands $[Pd(dppp)L_2]^{2+}$ concomitant with again the small monocationic complex $\{[Pd(dppp)]OTf\}^+$ at m/z 667. The preferred non-symmetric cleavage of the triply charged aggregate thus reduces the charge density in the dication compared to the hypothetical symmetrical alternative. In a subsequent process, only induced at slightly higher collision energies (Figure 2c), $[Pd(dppp)\,L]_2]^{2+}$ at m/z 773 loses one of the two ligands L yielding the dication $[Pd(dppp)L]^{2+}$ at m/z 516.

The same ion is also the primary fragmentation product of the quadruply charged rhomb (Figure 2d) which again splits

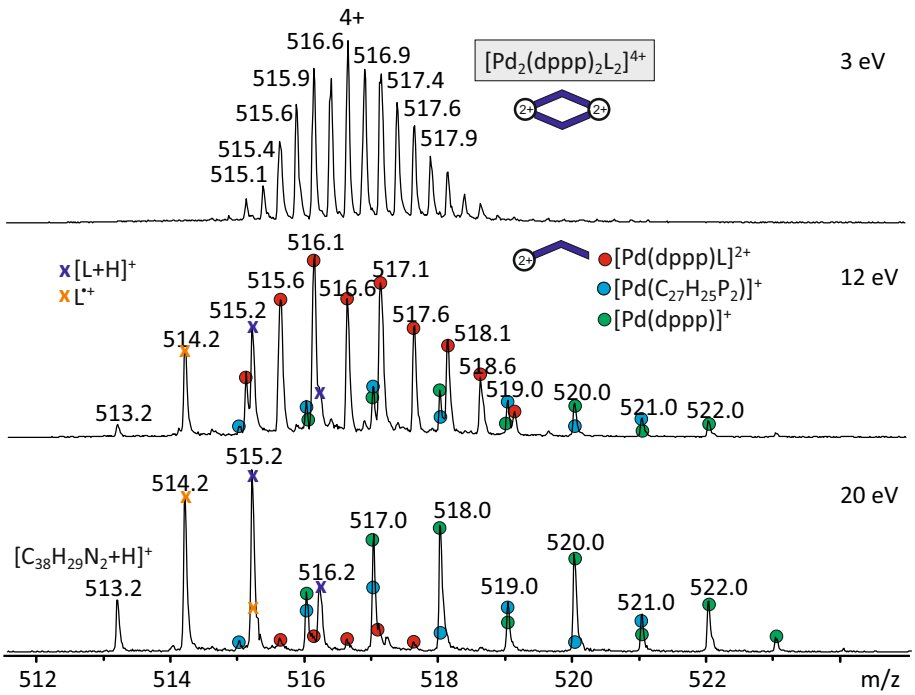

Figure 3. Isotope patterns and superposed signals around m/z 516 in the CID mass spectra shown in Figures 2 and 4 measured at the indicated collision energy voltages

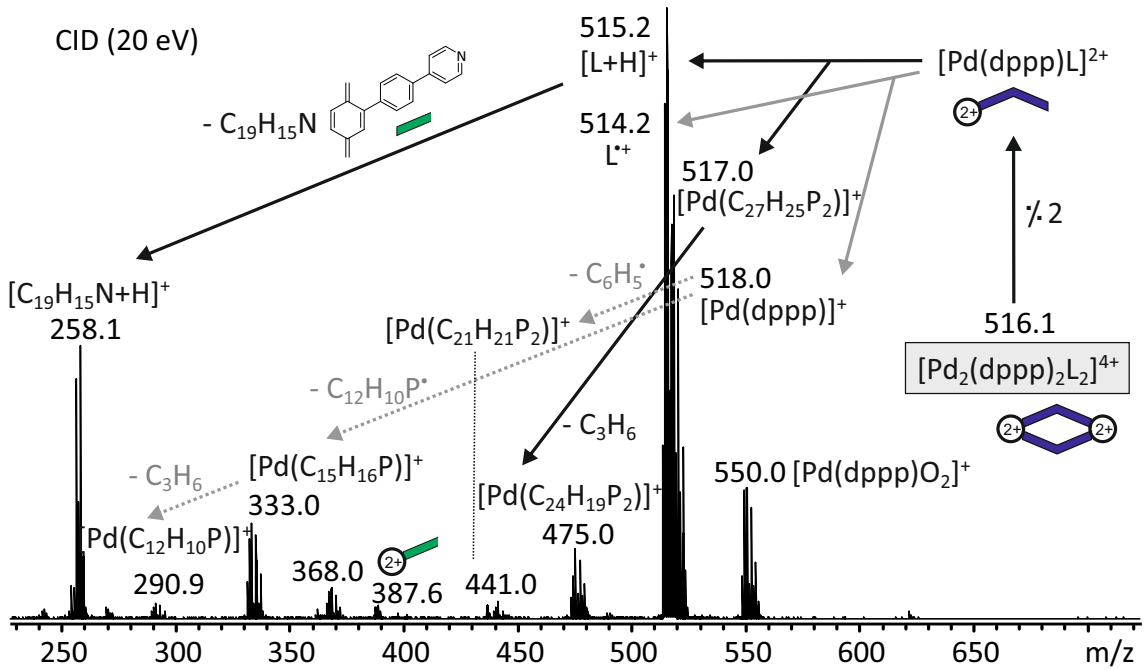

Figure 4. CID-mass spectrum of mass-selected $[Pd_2(dppp)_2L_2]^{4+}$ at *m/z* 516.6 at a collision energy voltage of 20 eV measured with the Q/TOF mass spectrometer. *m/z* 514–518 is a superposition of several ions, see Figure 3. Fragmentation pathways indicated with unbroken arrows are verified by CID spectra of ions generated independently (Figures 5 and 6). Note that the structure of the neutral fragment $C_{19}H_{15}N$ cannot be probed experimentally

symmetrically—very similar to the behavior of the doubly charged rhomb, but without anions. The subsequent fragmentation of $[Pd(dppp)L]^{2+}$ at *m/z* 516 is tricky to analyze due to strongly superposing signals. Clearly, both the mass-selected quadruply-charged rhomb as well as its main primary fragmentation product have the same *m/z* 516.1. Unfortunately, also the secondary fragmentation product $[Pd(C_{27}H_{25}P_2)]^+$ at *m/z* 517.0 and the protonated ligand $[L+H]^+$ at *m/z* 515.2 appear in the same region (Figure 3). The mass resolution of our instruments is sufficiently high to distinguish these signals, but the mass-selection window cannot be reduced as low as needed to probe the subsequent fragmentations separately.

However, careful analysis of the spectra obtained also at higher collision energies (Figures 3 and 4) reveals some fascinating unexpected behavior. The fragmentation pattern of $[Pd(dppp)L]^{2+}$ thus consists of three major competing pathways. The maybe most expected path is a charge-separating acid-base reaction leading to the protonated ligand $[L+H]^+$ at *m/z* 515 and a Pd-complex bearing a deprotonated dppp ligand $[Pd(C_{27}H_{25}P_2)]^+$ at *m/z* 517 (black arrows in Figure 4). The latter ion can be generated independently without disturbing superpositions (Figure 5) via loss of HOTf upon CID of $\{[Pd(dppp)]OTf\}^+$ [44, 52, 53]. The deprotonation probably occurs at one of the phenyl rings because the intact propylene bridge is split off during the following fragmentation via propene loss. A second charge-separating fragmentation pathway of $[Pd(dppp)L]^{2+}$ shows that the ligand L is not redox-innocent: $[Pd(dppp)L]^{2+}$ fragments into the ligand radical cation $L^{\bullet+}$ at *m/z* 514 and the unusual complex $[Pd(dppp)]^+$ at *m/z* 518 (gray arrows in Figure 4). This ion might best be understood as a complex of Pd^0 with a $(dppp)^{\bullet+}$ ligand formed via intramolecular metal reduction by a redox-active ligand in the gas phase [29]. Addition of molecular oxygen (*m/z* 550) as well as several radical losses from $[Pd(dppp)]^+$ nicely corroborate its open-shell nature.

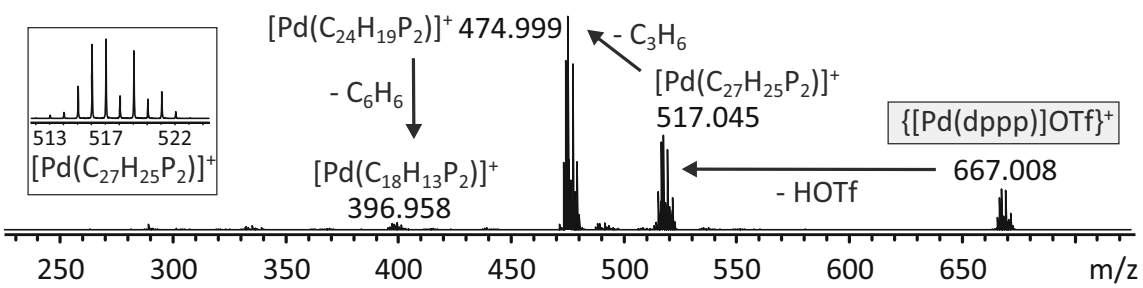

Figure 5. CID-mass spectrum of mass-selected $\{[Pd(dppp)]OTf\}^+$ at *m/z* 667 at a collision energy voltage of 25 eV measured with the Q/TOF mass spectrometer in ESI-positive mode when spraying $[Pd(dppp)](OTf)_2$ in CH_3CN. The inset shows the region measured around *m/z* 515 with the clean isotope pattern of $[Pd(C_{27}H_{25}P_2)]^+$

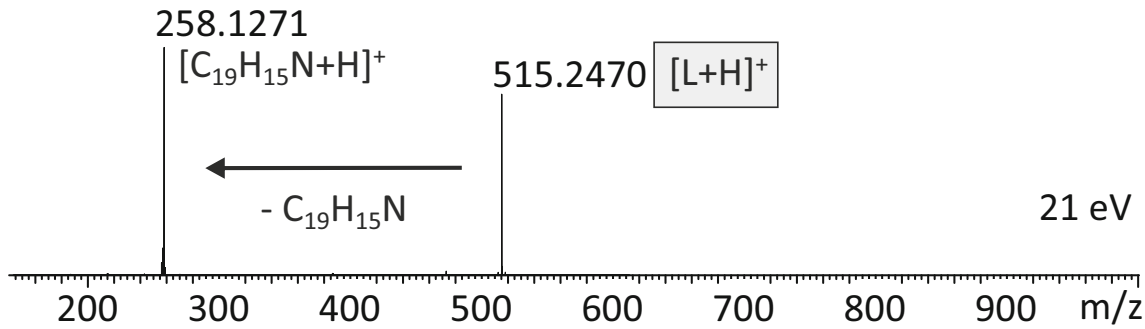

Figure 6. CID-mass spectrum of mass-selected $[L + H]^+$ at *m/z* 515 at a collision energy voltage of 21 eV measured at the Orbitrap XL mass spectrometer in ESI-positive mode from CH_3CN. Calculated exact masses: $[C_{19}H_{16}N]^+$: 258.1277; $[C_{38}H_{31}N_2]^+$: 515.2482

Finally, a third fragmentation pathway of $[Pd(dppp)L]^{2+}$ is less intense, but clearly visible, particularly at lower collision energies (Figure 2d). The ligand is centrally cleaved into two parts of the elemental composition $C_{19}H_{15}N$, one of which stays bound to the dicationic metal (*m/z* 387.6). This is an extremely intriguing process as the rupture of two weak, but covalent bonds in the [2.2]paracyclophane core of the ligand obviously is preferred over cleavage of the metallo-supramolecular Pd-pyridine dative bond—which in all our previously studied cases was the first bond broken upon CID and thus was assumed to be the weakest bond in the aggregate. The ligand rupture is only observed for the doubly charged ion $[Pd(dppp)L]^{2+}$, but not for its singly charged analogue $\{[Pd(dppp)L](OTf)\}^+$ which only loses the full ligand (Figure 2a). One thus could speculate that the remaining half ligand is needed as a kind of internal solvation of the doubly charged ion $[Pd(dppp)]^{2+}$ in the gas phase. Given the outstanding role palladium plays in metalorganic catalysis to form and cleave C–C bonds, it seemed plausible at first sight that the metal could promote the cleavage of the ligand. This however is not necessarily the case: CID of the simple protonated ligand $[L+H]^+$ indeed shows the very same fragmentation (Figure 6).

Conclusion

Self-assembled metallo-supramolecular rhombs based on an unusual chiral [2.2]paracyclophane bis(pyridine) ligand can be transferred into the gas phase via ESI under very soft ionization conditions. CID fragmentation patterns of the multiply charged aggregates $[Pd_2(dppp)_2L_2](OTf)_{4-n}]^{n+}$ $(n = 2 - 4)$ depend on the charge state of the respective mass-selected ion. The rather simple fragmentation pattern observed for the doubly charged ions are in full accordance with expectations based on previous results reported for metallo-supramolecular rhombs and squares. The triply charged species cleaves unsymmetrically which can be rationalized by a preferred formation of ions with low charge density. In both cases, only weak metal-pyridine dative bonds are cleaved. CID of the quadruply charged rhomb reveals a more complex fragmentation behaviour that inter alia includes ligand oxidation to the radical cation. In addition, an intriguingly facile cleavage of the central covalent bonds of the [2.2]paracyclophane ligand takes place which is even preferred over rupture of the weak dative pyridine-Pd bond.

Acknowledgements

We thank the Studienstiftung des deutschen Volkes for a doctoral scholarship and the Bonn International Graduate School of Chemistry for an international research scholarship (J.A.), and the Deutsche Forschungsgemeinschaft (SFB 813) for financial support.

References

1. Chakrabarty, R., Mukherjee, P.S., Stang, P.J.: Supramolecular coordination: self-assembly of finite two- and three-dimensional ensembles. Chem. Rev. **111**, 6810–6918 (2011)
2. Amouri, H., Desmarets, C., Moussa, J.: Confined nanospaces in metallocages: guest molecules, weakly encapsulated anions, and catalyst sequestration. Chem. Rev. **112**, 2015–2041 (2012)
3. Debata, N.B., Tripathy, D., Chand, D.K.: Self-assembled coordination complexes from various palladium(II) components and bidentate or polydentate ligands. Coord. Chem. Rev. **256**, 1831–1945 (2012)
4. Cook, T.R., Zheng, Y.R., Stang, P.J.: Metal–organic frameworks and self-assembled supramolecular coordination complexes: comparing and contrasting the design, synthesis, and functionality of metal–organic materials. Chem. Rev. **113**, 734–777 (2013)
5. Cook, T.R., Stang, P.J.: Recent developments in the preparation and chemistry of metallacycles and metallacages via coordination. Chem. Rev. **115**, 7001–7045 (2015)
6. Winter, A., Schubert, U.S.: Synthesis and characterization of metallo-supramolecular polymers. Chem. Soc. Rev. **45**, 5311–5357 (2016) and references cited therein
7. Saha, M.L., Schmittel, M.: From 3-fold completive self-sorting of a nine-component library to a seven-component scalene quadrilateral. J. Am. Chem. Soc. **135**, 17743–17746 (2013)
8. Wang, S.-Y., Fu, J.-H., Liang, Y.-P., He, Y.-J., Chen, Y.-S., Chan, Y.-T.: Metallo-supramolecular self-assembly of a multicomponent ditrigon based on complementary Terpyridine ligand pairing. J. Am. Chem. Soc. **138**, 3651–3654 (2016)
9. Yao, Y., Chakraborty, S., Zhu, S., Endres, K.K., Xie, T.-Z., Hong, W., Manandhar, E., Moorefield, C.N., Wesdemiotis, C., Newkome, G.R.: Stepwise, multicomponent assembly of a molecular trapezoid possessing three different metals. Chem. Commun. **53**, 8038–8041 (2017)
10. Seperpour, H., Lal Saha, M., Stang, P.J.: Fe–Pt twisted heterometallic bicyclic supramolecules via multicomponent self-assembly. J. Am. Chem. Soc. **139**, 2553–2556 (2017)
11. Osowska, K., Miljanić, O.S.: Kinetic and thermodynamic self-sorting in synthetic systems. Synlett (12), 1643–1648 (2011). https://doi.org/10.1055/s-0030-1260815
12. Safont-Sempere, M.M., Fernández, G., Würthner, F.: Self-sorting phenomena in complex supramolecular systems. Chem. Rev. **111**, 5784–5814 (2011)
13. Lal Saha, M., Schmittel, M.: Degree of molecular self-sorting in multi-component systems. Org. Biomol. Chem. **10**, 4651–4684 (2012)
14. He, Z., Jiang, W., Schalley, C.A.: Intergrative self-sorting: a versatile strategy for the construction of complex supramolecular architectures. Chem. Soc. Rev. **44**, 779–789 (2015)

15. Wei, P., Yan, X., Huang, F.: Supramolecular polymers constructed by orthogonal self-assembly based on host–guest and metal–ligand interactions. Chem. Soc. Rev. **44**, 815–832 (2015)
16. Angurell, I., Ferrer, M., Gutiérrez, A., Martínez, M., Rodríguez, L., Rossell, O., Engeser, M.: Antisymbiotic self-assembly and dynamic behavior of metallamacrocycles with allylic corners. Chem. Eur. J. **16**, 13960–13964 (2010)
17. Angurell, I., Ferrer, M., Gutiérrez, A., Martínez, M., Rocamora, M., Rodríguez, L., Rossell, O., Lorenz, Y., Engeser, M.: Kinetico-mechanistic insights on the assembling dynamics of allyl-cornered metallacycles: the Pt-N_{py} bond is the keystone. Chem. Eur. J. **20**, 14473–14487 (2014)
18. Schalley, C.A.: Molecular recognition and supramolecular chemistry in the gas phase. Mass Spectrom. Rev. **20**, 253–309 (2001)
19. Yamaguchi, K.: Cold-spray ionization mass spectrometry: principle and applications. J. Mass Spectrom. **38**, 473–490 (2003)
20. Schalley, C.A., Springer, A.: Mass spectrometry and gas phase chemistry of non-covalent complexes. Wiley, New York (2009)
21. Cera, L., Schalley, C.A.: Supramolecular reactivity in the gas phase: investigating the intrinsic properties of non-covalent complexes. Chem. Soc. Rev. **43**, 1800–1812 (2014)
22. Wesdemiotis, C.: Multidimensional mass spectrometry of synthetic polymers and advanced materials. Angew. Chem. Int. Ed. **56**, 1452–1464 (2017)
23. Ferrer, M., Gutiérrez, A., Mounir, M., Rossell, O., Ruiz, E., Rang, A., Engeser, M.: Self-assembly reactions between the cis-protected metal corners $(N{-}N)M^{II}$ (N−N = ethylenediamine, 4,4′-substituted 2,2′-bipyridine; M = Pd, Pt) and the fluorinated edge 1,4-bis(4-pyridyl)tetrafluorobenzene. Inorg. Chem. **46**, 3395–3406 (2007)
24. Schmittel, M., He, B., Fan, J., Bats, J.W., Engeser, M., Schlosser, M., Deiseroth, H.: Cap for copper(I) ions! Metallosupramolecular solid and solution state structures on the basis of the dynamic tetrahedral $[Cu(phenAr_2)(py)_2]^+$ motif. Inorg. Chem. **48**, 8192–8200 (2009)
25. Albrecht, M., Fiege, M., Kögerler, P., Speldrich, M., Fröhlich, R., Engeser, M.: Magnetic coupling in enantiomerically pure trinuclear helicate-type complexes formed by hierarchical self-assembly. Chem. Eur. J. **16**, 8797–8804 (2010)
26. Neogi, S., Schnakenburg, G., Lorenz, Y., Engeser, M., Schmittel, M.: Implications of stoichiometry-controlled structural changeover between heteroleptic trigonal $[Cu(phenAr_2)(py)]^+$ and tetragonal $[Cu(phenAr_2)(py)_2]^+$ motifs for solution and solid-state supramolecular self-assembly. Inorg. Chem. **51**, 10832–10841 (2012)
27. Neogi, S., Lorenz, Y., Engeser, M., Samanta, D., Schmittel, M.: Heteroleptic metallosupramolecular racks, rectangles, and trigonal prisms: stoichiometry-controlled reversible interconversion. Inorg. Chem. **52**, 6975–6984 (2013)
28. Hovorka, R., Hytteballe, S., Piehler, T., Meyer-Eppler, G., Topić, F., Rissanen, K., Engeser, M., Lützen, A.: Self-assembly of metallosupramolecular rhombi from chiral concave 9,9′-spirobifluorene-derived bis(pyridine) ligands. Beilstein J. Org. Chem. **10**, 432–441 (2014)
29. Gütz, C., Hovorka, R., Struch, N., Bunzen, J., Meyer-Eppler, G., Qu, Z.-W., Grimme, S., Cetina, M., Topić, F., Rissanen, K., Engeser, M., Lützen, A.: Enantiomerically pure trinuclear helicates via diastereoselective self-assembly and characterization of their redox chemistry. J. Am. Chem. Soc. **136**, 11830–11838 (2014)
30. Hovorka, R., Meyer-Eppler, G., Piehler, T., Hytteballe, S., Engeser, M., Topić, F., Rissanen, K., Lützen, A.: Unexpected self-assembly of a homochiral metallosupramolecular M_4L_4 catenane. Chem. Eur. J. **20**, 13253–13258 (2014)
31. Struch, N., Bannwarth, C., Ronson, T.K., Lorenz, Y., Mienert, B., Wagner, N., Engeser, M., Bill, E., Puttreddy, R., Rissanen, K., Beck, J., Grimme, S., Nitschke, J.R., Lützen, A.: An octanuclear metallosupramolecular cage designed to exhibit spin-crossover behavior. Angew. Chem. Int. Ed. **56**, 4930–4935 (2017)
32. Chan, Y.-T., Li, X., Yu, J., Carri, G.A., Moorefield, C.N., Newkome, G.R., Wesdemiotis, C.: Design, synthesis, and traveling wave ion mobility mass spectrometry characterization of iron(II)– and ruthenium(II)–terpyridine metallomacrocycles. J. Am. Chem. Soc. **133**, 11967–11976 (2011)
33. Li, X., Chan, Y., Newkome, G.R., Wesdemiotis, C.R.: Gradient tandem mass spectrometry interfaced with ion mobility separation for the characterization of supramolecular architectures. Anal. Chem. **83**, 1284–1290 (2011)
34. Guo, K., Guo, Z., Ludlow, J.M., Xie, T., Liao, S., Newkome, G.R., Wesdemiotis, C.: Characterization of metallosupramolecular polymers by top-down multidimensional mass spectrometry methods. Macromol. Rap. Commun. **36**, 1539–1552 (2015)
35. Zhang, Z., Wang, H., Wang, X., Li, Y., Song, B., Bolarinwa, O., Reese, R.A., Zhang, T., Wang, X.-Q., Cai, J., Xu, B., Wang, M., Liu, C., Yang, H.-B., Li, X.: Supersnowflakes: stepwise self-assembly and dynamic exchange of rhombus star-shaped supramolecules. J. Am. Chem. Soc. **139**, 8174–8185 (2017)
36. Brusilowskij, B., Neubacher, S., Schalley, C.A.: A double intramolecular cage contraction within a self-assembled metallo-supramolecular bowl. Chem. Commun. 785–787 (2009). https://doi.org/10.1039/B819412B
37. Brusilowskij, B., Dzyuba, E.V., Troff, R.W., Schalley, C.A.: Effects of subtle differences in ligand constitution and conformation in metallo-supramolecular self-assembled polygons. Dalton Trans. **40**, 12089–12096 (2011)
38. Brusilowskij, B., Dzyuba, E.V., Troff, R.W., Schalley, C.A.: Thermodynamically controlled self-sorting of hetero-bimetallic metallo-supramolecular macrocycles: what a difference a methylene group makes! Chem. Commun. **47**, 1830–1832 (2011)
39. Rodríguez, L., Lima, J.C., Ferrer, M., Rossell, O., Engeser, M.: 3D au–ag heterometallic supramolecular cage: triplet capture by heavy atom effect. Inorg. Chim. Acta. **381**, 195–202 (2012)
40. Gütz, C., Hovorka, R., Klein, C., Jiang, Q.-Q., Bannwarth, C., Engeser, M., Schmuck, C., Assenmacher, W., Mader, W., Topić, F., Rissanen, F., Grimme, S., Lützen, A.: Enantiomerically pure $[M_6L_{12}]$ or $[M_{12}L_{24}]$ polyhedra from flexible bis(pyridine) ligands. Angew. Chem. Int. Ed. **53**, 1693–1698 (2014)
41. Sleno, L., Volmer, D.A.: Ion activation methods for tandem mass spectrometry. J. Mass Spectrom. **39**, 1091–1112 (2004)
42. Gross, J.H.: Mass spectrometry. A textbook. Springer, Berlin (2004)
43. F. W. McLafferty, F. Turecek, Interpretation of mass spectra, 4th edn. University Science Books (1993).
44. Ferrer, M., Gutiérrez, A., Rodríguez, L., Rossell, O., Ruiz, E., Engeser, M., Lorenz, Y., Schilling, R., Gómez-Sahl, P., Martín, A.: Self-assembly of heterometallic metallomacrocycles via Ditopic fluoroaryl gold(I) organometallic metalloligands. Organometallics. **31**, 1533–1545 (2012)
45. Cooks, R.G., Patrick, J.S., Kotiaho, T., McLuckey, S.A.: Thermochemical determinations by the kinetic method. Mass Spec. Rev. **13**, 287–339 (1994)
46. Cooks, R.G., Wong, P.S.H.: Kinetic method of making thermochemical determinations: advances and applications. Acc. Chem. Res. **31**, 379–386 (1998)
47. Wu, H.F., Brodbelt, J.S.: Comparison of the orders of gas-phase basicities and ammonium ion affinities of polyethers by the kinetic method and ligand exchange technique. J. Am. Soc. Mass Spectrom. **4**, 718–722 (1993)
48. Schröder, D., Schwarz, H.: Ligand effects as probes for mechanistic aspects of remote C-H bond activation by iron(I) cations in the gas phase. J. Organomet. Chem. **504**, 123–135 (1995)
49. Rodgers, M.T., Armentrout, P.B.: Cationic noncovalent interactions: energetics and periodic trends. Chem. Rev. **116**, 5642–5687 (2016)
50. Lorenz, Y., Gutiérrez, A., Ferrer, M., Engeser, M.: Bond dissociation energies of metallosupramolecular building blocks: insight from fragmentation of selectively self-assembled heterometallic metallo-supramolecular aggregates. Inorg. Chem. **57**, 7346–7354 (2018)
51. Stang, P.J., Cao, D.H.: Transition metal based cationic molecular boxes. Self-assembly of macrocyclic platinum(II) and palladium(II) tetranuclear complexes. J. Am. Chem. Soc. **116**, 4981–4982 (1994)
52. Schalley, C.A., Müller, T., Linnartz, P., Witt, M., Schäfer, M., Lützen, A.: Mass spectrometric characterization and gas-phase chemistry of self-assembling supramolecular squares and triangles. Chem. Eur. J. **8**, 3538–3551 (2002)
53. Engeser, M., Rang, A., Ferrer, M., Gutierrez, A., Baytekin, H.T., Schalley, C.A.: Reactivity of self-assembled supramolecular complexes in the gas phase: a supramolecular neighbor group effect. Int. J. Mass Spectrom. **255/256**, 185–194 (2006)
54. Anhäuser, J., Puttreddy, R., Lorenz, Y., Schneider, A., Engeser, M., Rissanen, K., Lützen, A.: Chiral self-sorting behaviour of [2.2]paracyclophane-based bis(pyridine) ligands. Org. Chem. Front. **6**, 1226–1235 (2019). https://doi.org/10.1039/C9QO00155G
55. Additional new signals in the range *m/z* 500-660 can be assigned to mononuclear Pd-complexes with some other anions which stem from previous LC-MS runs performed on the same instrument.